

DEVELOPMENT OF AN INDEPENDENT HIP DRIVE FOR A 2D BIPED
WALKING MACHINE

By

Craig Rooney

Submitted to the graduate degree program in Mechanical Engineering and the
Graduate Faculty of the University of Kansas in partial fulfillment of the
requirements for the degree of Master of Science.

Terry N. Faddis, Chairperson

Dr. Depcik, Committee Member

Robert C. Umholtz, Committee Member

Date Defended: 7/24/12

The Thesis Committee for Craig Rooney

Certifies that this is the approved version of the following thesis:

DEVELOPMENT OF AN INDEPENDENT HIP DRIVE FOR 2D BIPED
WALKING MACHINE

Terry N. Faddis, Chairperson

Date approved: 7/27/12

ABSTRACT

Bipedal robots have advantages over wheeled or multi-legged robots because they require fewer footholds for locomotion and can traverse a larger percentage of Earth's terrain including discontinuous or rough terrain. The Intelligent Systems and Automation Laboratory (ISAL) at the University of Kansas has developed a two dimensional (2D) biped walker, nicknamed the Jaywalker, in order to study the requirements necessary for a bipedal robot to traverse uneven terrain and successfully regain stability after encountering perturbations.

In order to maintain stability over rough terrain, the robot must be capable of controlling each leg independently ensuring foot placement on stable footholds. Foot placement is, therefore, critical for stability since a misstep can cause the robot to slip or distribute its weight unevenly on the foothold causing it to become unstable and fall over. An independent drive system was incorporated into the robot's hip that directly couples the hip motors to the legs, eliminates flexible connections in the power transmission system that can add unnecessary errors, and increases the leg rotation resolution, which all increase the robot's foot placement accuracy.

Testing was performed to prove the independent hip drive design can operate within human gait parameters, has the same or better range of motion as a human, and is capable of taking a stable step.

ACKNOWLEDGEMENT

I would like to thank my advisor Dr. Terry Faddis for guiding me during my research and design. His extensive knowledge and experience has allowed this project to be a success. I would also like to thank my defense committee, Dr. Chris Depcik and Professor Robert C. Umholtz for their efforts.

This project would not have been possible without help and advice from Dr. Bryce Baker and Gavin Strunk who have given me support throughout this project.

A special thanks to my parents Tim and Cindy and brother C.J. for their advice and support.

TABLE OF CONTENTS

LIST OF FIGURES	vii
1. Outline.....	1
2. Literature Review.....	2
2.1 Introduction.....	2
2.2 References.....	8
3. Introduction.....	10
3.1 Introduction.....	10
3.2 References.....	11
4. Background and Significance	12
4.1 Introduction.....	12
4.2 Ratchet Hip Design Problems/Limitations	13
4.3 References.....	15
5. Design of Independent Hip Drive	16
5.1 Introduction.....	16
5.2 Torque Analysis	18
5.3 Spur Gear Selection	19
5.4 Drive Shaft Design.....	20
5.5 Stepper Motor/Drive Shaft Mounting	20
5.6 Leg Clevis Design.....	21
5.7 Packaging Concerns.....	22
5.8 Weight Comparison	24
5.9 References.....	25
6. Manufacturing.....	27
6.1 Introduction.....	27
6.2 Difficulties during Manufacturing	27
6.3 Manufacturing Improvements.....	33
7. Assembly.....	35
7.1 Introduction.....	35

7.2 Difficulties during Assembly	36
8. Test Methods	37
8.1 Test Method for Robot Range of Motion	37
8.2 Test Method for Open Loop Stable Step Length	37
8.3 Test Method for Robot Walking at Human Gait Parameters	37
8.4 References	38
9. Test Results	39
9.1 Test Results for Robot Range of Motion	39
9.2 Test Results for Open Loop Stable Step Length	39
9.3 Test Results for Robot Walking at Human Gait Parameters	39
9.4 References	40
10. Conclusions	41
11. Future Recommendations and Testing	42
A. APPENDIX A: Maximum Motor Torque to Raise Hip to 30°	45
B. APPENDIX B: Bill of Materials	46
C. APPENDIX C: Manufacturing Drawings	47
D. APPENDIX D: Stress Analysis for Leg Clevis Weight Reduction	55
E. APPENDIX E: Keyway Shear Stress Analysis	56
F. APPENDIX F: Jaywalker Step Test Screenshots	57
G. APPENDIX G: Appendix References	59

LIST OF FIGURES

FIGURE 1: The A.M.P. robot – uses wheels for locomotion requiring a continuously smooth path	2
FIGURE 2: The S.W.O.R.D.S. robot – uses tracks for locomotion requiring a semi-continuous path.....	2
FIGURE 3: The BigDog robot – has four legs capable of taking discrete steps over rough terrain	3
FIGURE 4: The Human Gait Cycle – divided into sub phases	4
FIGURE 5: IPM Free Body Diagram	5
FIGURE 6: Honda ASIMO’s ZMP control strategy	6
FIGURE 7: Ratchet/pawl hip design with single center-mounted motor/gear train assembly	12
FIGURE 8: Ratchet/pawl locking mechanism located in robot thigh.	12
FIGURE 9: Flexible connections – the ratchet/pawl hip’s six flexible transmission connections shown	14
FIGURE 10: Independent hip drive design - uses a motor/gear train assembly for each outer leg.	16
FIGURE 11: Independent hip drive’s three transmission connections shown	16
FIGURE 12: Snap ring locations on leg drive shaft.	20
FIGURE 13: Top pelvis mount - removed and replaced by second bearing carrier (shown in phantom).....	20
FIGURE 14: Weight removed from inside leg clevis	21
FIGURE 15: Organized electrical and pneumatic connectors	22
FIGURE 16: Weight comparison of ratchet/pawl and independent hip drive.....	24
FIGURE 17: Bearing holes milled too deep.	28
FIGURE 18: Weight removed from leg clevis due to machining error.....	30
FIGURE 19: Free body diagram of IPM	43

1. Outline

The discussion will begin by stating the importance of studying bipedal robots and then describing the human walking gait and two methods to analyze the stability of active walkers. This will lead into how the hip is crucial to the stability of the walking robot along with the factors that need to be considered when transitioning the robot hip from partially passive to fully active, which is required to walk on uneven terrain.. Next, the Jaywalker's previous passive hip design will be discussed with its design failures followed by the requirements necessary for the design of the new independent hip drive system and how it was designed according to the human gait cycle. This will be followed by test results and conclusions in order to prove the independent hip drive design operates within human walking gait parameters.

2. Literature Review

2.1 Introduction

Robots are developed to make people's lives easier. They can perform tasks that are too repetitive, too dangerous, or too difficult for their human counterparts and usually perform these tasks more efficiently. Past terrain traversing robots have used wheels, tracks, or legs for movement.

Robots that use wheels like the A.M.P. robot (Figure 1) require a continuous smooth path



Figure 1: The A.M.P. robot - uses wheels for locomotion requiring a continuously smooth path [14]

to move since a discontinuous surface would either prevent further motion or could cause the robot's wheels to distribute its weight unevenly causing it to become unstable.



Robots that use tracks such as the S.W.O.R.D.S. (Figure 2) can be

Figure 2: The S.W.O.R.D.S. robot - uses tracks for locomotion requiring a semi-continuous path. [1]

used in a wider range of environments, compared to wheeled vehicles, but still require a semi-continuous locomotion path. Multi-legged robots such as the Boston

Dynamics BigDog quadruped (Figure 3) can traverse a larger percentage of Earth's surface because they have the ability to take discrete steps and, therefore, can walk on smooth and rough terrain. The drawback of quadruped and hexapods (six legged robots) are that they require two to three footholds to be in close proximity [3] at any given time to allow walking, and because each leg must be powered for actuation, they have to be tethered to a continuous power source otherwise they have poor battery life [4]. A more ideal robot for walking on uneven terrain would be bipedal (two legs). They have the ability to traverse a larger percentage of Earth's terrain because they take discrete steps that require only two footholds to be in close proximity [3].

In order to develop a bipedal robot, the human walking cycle or "gait cycle" must first be explained. The gait cycle can be described as the repetitive motion that occurs during walking,

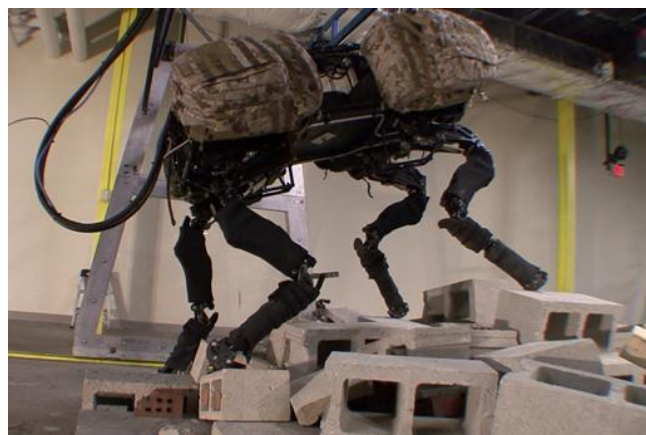


Figure 3: The BigDog - has four legs capable of taking discrete steps over rough terrain [2].

beginning with the heel strike of one foot and ending with the heel strike of the same foot. This motion can be further broken down into two phases; Stance and Swing (Figure 4). The Stance phase begins when the heel of Leg 1 initially contacts the ground. As the human's center of mass moves forward and the planted foot rolls from heel to full foot contact, the motion enters the "Loading Response" phase. During this time, Leg 2 enters the "Pre-swing" phase. Leg 2 then transitions into "Swing Phase"

while Leg 1 enters “Mid-stance”, which occurs when all body weight is placed on this leg. “Terminal Stance” begins when only the toe is in floor contact, termed “toe off,” and occurs just before heel strike of the swing leg. Leg 1 enters “Pre-swing” after heel strike of Leg 2 and then Leg 2 transitions into the “Loading Response” phase. Leg 1 then enters “Swing Phase” and ends with heel strike, completing the first cycle. This sequence is repeated allowing the human to walk [3].

A simple model used to describe the stability of human walking is the inverted pendulum model. This model can

easily be explained by assuming a walking model with a point mass at the hip and two massless rigid legs spread apart. As Leg 1 transitions from the “Initial Contact” (Figure

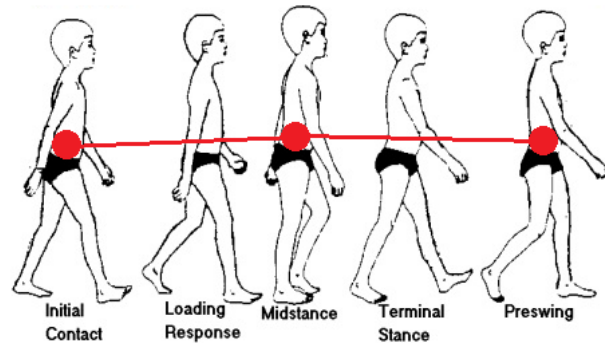


Figure 4: The Human Gait Cycle - divided into sub phases [13].

4) into the “Midstance” phase, the hip mass is raised vertically

increasing potential energy, and the velocity of the hip decreases, decreasing kinetic energy. The transition from the “Midstance” phase to the “Preswing” phase lowers the hip mass, decreasing potential energy, and the velocity of the hip increases, increasing kinetic energy. This is equivalent to a swinging pendulum where kinetic energy is converted into potential energy and back to kinetic energy [5]. McGeer develops an analytical method to describe the inverted pendulum model with a two dimensional (2-D) passive walker capable of walking down an inclined surface with no input energy other than gravity. The inverted pendulum model is attractive

because it allows the stability equation for a passive walker to be formed relatively simply and with high efficiency using only three parameters (foot radius, center of mass height, and radius of gyration). The eigenvalues for this equation are then solved and indicate stability of the system [6].

The problems with this method, as described by McGeer, are that it assumes all body mass as a single point mass located at the hip (Figure 5) and an infinitesimally small mass located at the feet. This simplifies the equations because the stance leg is not affected by the inertial effects of the swing leg [7], but in reality, the legs of an active walker have substantial weight due to actuators. The method also uses rigid, inelastic legs in order to conserve angular momentum and maintain 100% energy recovery between leg strikes when transferring from kinetic to potential energy or vice versa. This assumption simplifies the equations, but according to Farley [5] only 60-70% of energy is actually conserved in this method. Lastly, because no lateral or rocking side-to-side movement is allowed as the swing leg passes vertical, a minimal change in leg inertia is assumed when the foot contacts the ground. This is unrealistic because when the swing foot hits the ground a large change in leg inertia occurs, but this complicates the equations and is not

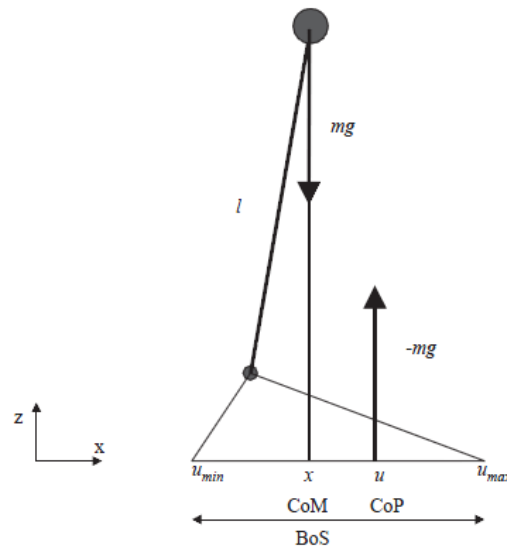


Figure 5: IPM free body diagram [15]

taken into account. This dynamic walker is called a limit cycle walker because unstable walking will converge to stable periodic walking regardless of minor perturbations. Because uneven terrain is non-periodic, a pure limit cycle walker is not capable of traversing uneven terrain [8].

Even though the inverted pendulum model makes large assumptions it does identify the driving factors necessary for bipedal walking. McGeer shows that stable walking can be accomplished for a certain range of step lengths and slope angles and in other situations unstable walking will converge to stable walking [9]. He does indicate that passive walkers are limited because they can only operate on slightly angled surfaces not more than a few degrees [10] before becoming unstable and falling over. Because the goal of the ISAL bipedal robot is to traverse uneven terrain and operate on inclined surfaces, it is necessary to incorporate an active hip. Parts of passive hip technology may be utilized in the future to lower energy consumption and to better mimic human walking.

Robots like the Honda ASIMO [11] use active hip control and sensors to keep their walking stable. ASIMO accomplishes stable walking by monitoring the location of the Zero Moment Point (ZMP) and reaction force at the contact foot. The ZMP is defined as the intersection point of the walking surface and the extended axis of the robot's inertial force originating from the center of mass. The total inertial force is the

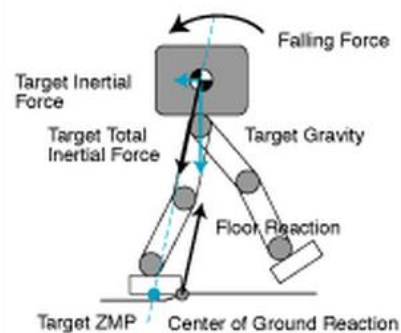


Figure 6: Honda ASIMO's ZMP control strategy [11].

combination of the accelerations/decelerations of walking and the force applied to the robot's center of mass due to Earth's gravity. When the extended axis of the reaction force located at the point where the robot's foot contacts the ground aligns with the total inertial force, walking is stable since no overall inertial force moment is generated (Figure 6). If the reaction force does not intersect the ZMP an overall moment is generated that causes ASIMO to become unstable and rotate forward or backward. ASIMO's software monitors the location of the ZMP and reaction force using its sensors and tries to adjust joint torques in the knees and feet to realign the inertial force and ZMP. Because the ZMP location is dependent on the inertial forces of the robot, which includes acceleration due to gravity and the robot's walking acceleration/deceleration, the robot's stability is dependent on the value of the hip mass. A smaller hip mass decreases the force applied to the robot's center of mass due to Earth's gravity and reduces the magnitude of the total inertial force. Reducing the hip mass lowers the center of mass height and reduces the necessary knee and ankle torques needed to realign the total inertial force and the contact foot reaction force when the robot becomes unstable since the moment arm between the knee and ankle motors and the center of mass is reduced. This was taken into account when attempting to reduce the mass of the new independent hip drive.

The drawback of using the ZMP is that it is too computationally intensive to calculate realignment trajectories when the robot encounters an un-expectant event. The robot tries to calculate the correct trajectory to re-stabilize, but may end up falling over because of its slower response time [11].

2.2 References

- [1] Sofge, Erik, 2009, "America's Robot Army: Are Unmanned Fighters Ready for Combat?," Popular Mechanics. <http://www.popularmechanics.com/technology/military/robots/4252643?page=2> (last visited on July, 17 2011).
- [2] Boston Dynamics, "BigDog – The Most Advanced Rough-Terrain Robot on Earth," at http://www.bostondynamics.com/robot_bigdog.html (last visited on July, 17 2011).
- [3] Baker, B., 2010, "Development of a hybrid powered 2D biped walking machine designed for rough terrain locomotion," Ph.D. thesis, the University of Kansas, Lawrence, KS, pp. 5.
- [4] Ruiz, M. Active hip actuation for walking biped with passive option. M.E. dissertation, University of Kansas, United States -- Kansas. Retrieved February 20, 2012, from Dissertations & Theses @ University of Kansas. (Publication No. AAT 1494802), pp. 2.
- [5] Farley, Claire T. and Ferris, Daniel P., 1998, "Biomechanics of Walking and Running: Center of Mass Movements to Muscle Action," at <http://www-personal.umich.edu/~ferrisd/Farley&Ferris,1998.pdf> (last visited on July, 17 2011), pp 259.
- [6] McGeer, T., 1990, "Passive dynamic walking," International Journal of Robotics Research, **9**(2), pp. 8-13.
- [7] McGeer, T., 1990, "Passive dynamic walking," International Journal of Robotics Research, **9**(2), pp. 7.
- [8] Baker, B., 2010, "Development of a hybrid powered 2D biped walking machine designed for rough terrain locomotion," Ph.D. thesis, the University of Kansas, Lawrence, KS, pp. 12.
- [9] McGeer, T., 1990, "Passive dynamic walking," International Journal of Robotics Research, **9**(2), pp. 12.
- [10] McGeer, T., 1990, "Passive dynamic walking," International Journal of Robotics Research, **9**(2), pp. 28.
- [11] Honda, "Evolution of Walking Technology – 2. Achieving Stable Walking," at <http://world.honda.com/ASIMO/history/technology2.html> (last visited March 12, 2012).

- [12] Baker, B., 2010, "Development of a hybrid powered 2D biped walking machine designed for rough terrain locomotion," Ph.D. thesis, the University of Kansas, Lawrence, KS, pp. 11.
- [13] Humphrey, Ellen, and Patton, Jim, "'Normal' Gait – Part of Kinesiology," at http://www.smpp.northwestern.edu/~jim/kinesiology/partA_introGait.ppt.pdf (last visited July 17, 2012). Department of Physical Therapy & Human Movement Sciences, Northwestern University, Medical School.
- [14] Yamamoto, Mike, 2008, "'A.M.P. Bot' wheels into robotic competition," at http://news.cnet.com/8301-17938_105-9972471-1.html (last visited July, 17 2011)
- [15] Hof, A. L., Gazendam, M. G. J., and Sinke, W. E., 2005, "The condition for dynamic stability," *Journal of Biomechanics*, 38(1), pp. 1-8.

3. Introduction

3.1 Introduction

The goal of the research performed in the Intelligent Systems and Automation Lab (ISAL) at the University of Kansas is to develop and test a bipedal robot that is capable of traversing uneven terrain by studying how it reacts to small perturbations. This is accomplished by incorporating sensors and flexibility into the robot's control system in order to allow it to react to the perturbation and re-stabilize itself before falling over. A future goal is to incorporate passive technologies into the active hip that allows the robot to better mimic human walking and lower its energy consumption allowing it to travel further distances [3].

There are currently robots under development that can traverse uneven terrain such as the Boston Dynamics Big Dog [1], but they have more than two legs, which require more footholds to be in close proximity and more energy for motion since each leg is actuated. A "human-like" robot would be ideal because it requires only two footholds to be in close proximity [2] and two legs to be powered, reducing overall energy consumption. A bipedal robot was selected over a wheeled robot or a robot with tracks because of the nature of uneven terrain. A wheeled robot and one with tracks must have a continuous smooth or slightly rough path to operate while a bipedal robot can take discrete steps [2]. Because uneven terrain is discontinuous and not a smooth path, a bipedal robot can traverse the terrain more effectively than a wheeled robot or one with tracks.

3.2 References

- [1] Boston Dynamics, “BigDog – The Most Advanced Rough-Terrain Robot on Earth,” at http://www.bostondynamics.com/robot_bigdog.html (last visited on July, 17 2011).
- [2] Baker, B., 2010, “Development of a hybrid powered 2D biped walking machine designed for rough terrain locomotion,” Ph.D. thesis, the University of Kansas, Lawrence, KS, pp. 5.
- [3] Baker, B., 2010, “Development of a hybrid powered 2D biped walking machine designed for rough terrain locomotion,” Ph.D. thesis, the University of Kansas, Lawrence, KS, pp. 12.

4. Background and Significance

4.1. Introduction

The previous biped hip design used a single center-mounted stepper motor and gear train assembly (Item 1 in Figure 7) connected to a single driveshaft (Item 2) via a timing belt (Item 3) and timing pulley (Item 4). The driveshaft was used to rotate the robot's outside legs simultaneously and at varying degrees to allow the robot to turn [1].

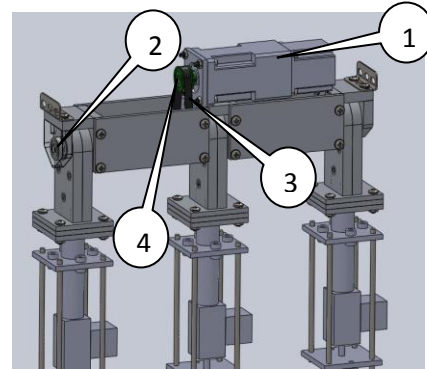


Figure 7: Ratchet/pawl hip design with single center-mounted motor/gear train assembly

A ratchet/pawl system was integrated into the upper portion of the robot's leg to lock the leg in place during swing phase. The ratchet/pawl system works by using a powerful servo motor (Item 1 in Figure 8) to engage/disengage a double-sided pawl (Item 2) against the rotating ratchet (Item 3) that rotates continuously with the stepper motor and driveshaft (Item 4)).

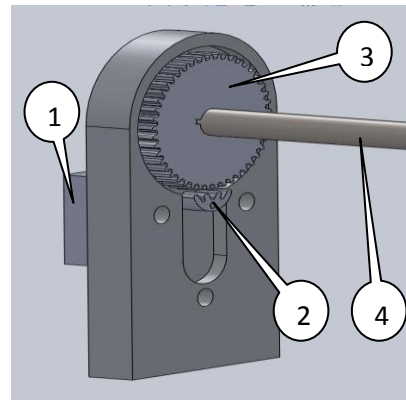


Figure 8: Ratchet/pawl locking mechanism located in robot thigh.

Engaging the pawl with the ratchet couples the leg and drivetrain together rotating the leg forward until a specific angle is reached [2]. At this specific angle, the control system causes the calf pneumatic

cylinder to extend, which extends the calf, straightening the leg. Once the control system senses heel strike of this swing leg, via a limit switch on the stance leg foot, the control system releases the pawl from the ratchet and rotates the pawl in the opposite direction until it engages the ratchet once more. This new pawl engagement causes the middle leg to rotate forward and the outer legs to be planted. This cycle repeats causing the robot to walk.

The drawbacks of the ratchet/pawl hip design are that it includes three design flaws that introduce unnecessary errors into the robot's foot placement. The first flaw is the large step resolution caused by the ratchet gear itself. Secondly, there are multiple flexible connections in the drivetrain that cause unnecessary errors, and lastly is the decoupling of the legs from the driveshaft.

4.2. Ratchet Hip Design Problems/Limitations

The ratchet/pawl hip design limits the robot's future walking capabilities. The ratchet/pawl system rotates the legs when the pawl engages the ratchet gear and according to Marc Ruiz, the previous hip ratchet system caused a leg and foot placement tolerance of 7.5^0 [3]. This is because 48-tooth ratchet gears were used, which means a tooth is located every 7.5^0 , and the leg pawl can only engage the ratchet and driveshaft in 7.5^0 intervals. With a 7.5^0 rotation at the hip, the distance the foot travels can be calculated by using trigonometry and the robot's leg length of 28.36". The distance each foot travels based only on the ratchet tooth quantity is 3.73". This means the Jaywalker's step length will vary by ± 3.73 " if the pawl misses engaging the ratchet by just one tooth. This can be the difference between

placing a foot on a stable foothold and missing the foothold and falling over. The independent hip drive design must improve upon this foot placement tolerance to allow accurate testing in the future.

The previous ratchet/pawl hip design also included six power transmission connections (Figure 9), two of which are flexible due to the interface between the two timing pulleys and timing belt used to couple the drivetrain and driveshaft together. All of these connections have unnecessary errors and the more connections involved, the more error introduced

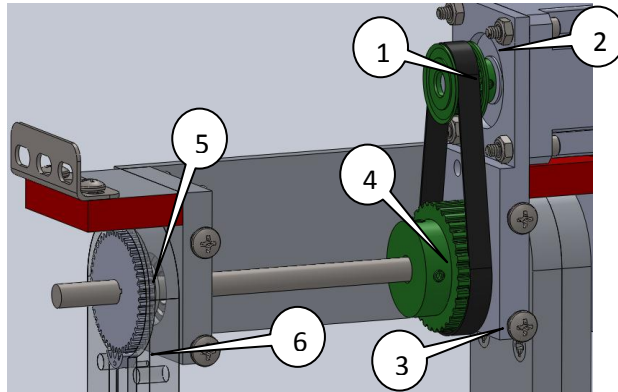


Figure 9: Flexible connections – the ratchet/pawl hip's six flexible transmission connections shown.

into the system and the less repeatable the results. One goal for the new hip design is to reduce the total number of power transmission connections and specifically remove all flexible connections since there is the possibility of belt stretch and slipping teeth that introduce the most error.

Decoupling the driveshaft from the legs further limits future walking abilities by making it more difficult for the control system to identify leg angle and, therefore, foot position for placing the foot on a stable foothold. Because the driveshaft rotates continuously and the pawl engages the ratchet right before the outside leg enters swing phase, the microprocessor cannot keep track of the leg angle with any precision since the hip stepper motor and leg servo motor do not communicate. Even if the

motors did communicate, the results still may not be accurate because of the limited number of teeth on the ratchet. The microcontroller may tell the pawl to engage the ratchet and think the resulting leg rotation angle is correct, but if the pawl tries to engage the ratchet and the two do not mesh immediately, the leg angle according to the microcontroller will not be the actual leg rotation causing the foot position to be incorrect. An encoder was planned to be incorporated on the driveshaft to fix the above problems, but because of miscommunication problems between it and the microcontroller the encoder was not implemented in testing [3].

4.3 References

- [1] Ruiz, M.. Active hip actuation for walking biped with passive option. M.E. dissertation, University of Kansas, United States -- Kansas. Retrieved February 20, 2012, from Dissertations & Theses @ University of Kansas. (Publication No. AAT 1494802), pp. 11.
- [2] Ruiz, M.. Active hip actuation for walking biped with passive option. M.E. dissertation, University of Kansas, United States -- Kansas. Retrieved February 20, 2012, from Dissertations & Theses @ University of Kansas. (Publication No. AAT 1494802), pp. 12.
- [3] Ruiz, M.. Active hip actuation for walking biped with passive option. M.E. dissertation, University of Kansas, United States -- Kansas. Retrieved February 20, 2012, from Dissertations & Theses @ University of Kansas. (Publication No. AAT 1494802), pp. 33.

5. Design of Independent Hip Drive

5.1 Introduction

The Independent Hip Drive design solves the above problems by incorporating a second VEXTRA PK266M-E2.0B stepper motor and 30:1 Micron EQ Series True

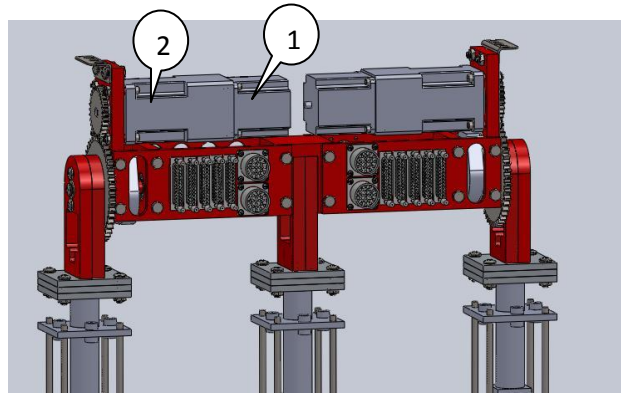


Figure 10: Independent hip drive design - uses a motor/gear train assembly for each outer leg.

Planetary gear train assembly and separate drive shafts to power and control each outer leg independently. The VEXTRA stepper motor (Item 1 in Figure 10) and Micron EQ gear train (Item 2) were selected because they provided the required torque at 17 rpm of each leg with an approximate 2.5 safety factor. This is explained in detail in Section 5.2. This addition solves the above problems by greatly reducing the foot position tolerance, removing flexible

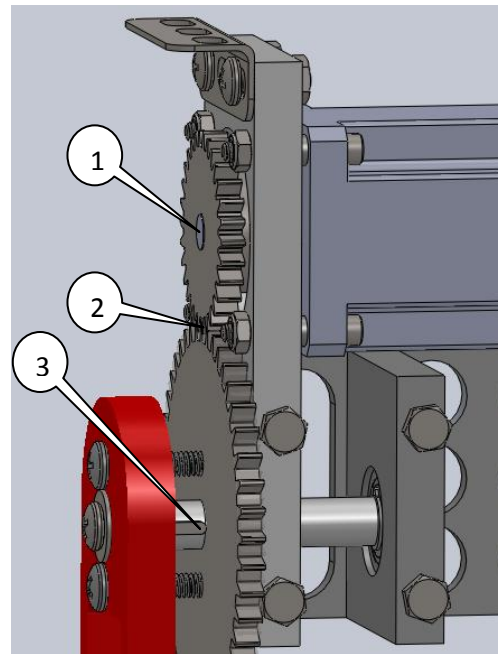


Figure 11: Independent hip drive's three transmission connections shown.

connections and reducing the power transmission connections from six to three (Figure 11), and directly coupling the stepper motor to each outer leg driveshaft allowing foot position to be easily and accurately obtained. The robot now has the ability to rotate its legs according to the 0.9° step angle [1] of the stepper motors and is not limited by the large resolution of the ratchet gear determined by the number of teeth on the gear. The 0.9° step angle translates into a step length accuracy of 0.007 inches compared to 3.73" with the ratchet/pawl hip design. This accuracy is solely based on the stepper motor capability and does not include slop due to the other transmission connections. The robot is now able to turn more accurately by rotating one outer leg more than the other with much more precision to allow more complicated testing with perturbations of various sizes, shapes, and textures in the future. The independent hip drive design can be seen in Figure 8.

One requirement for redesigning the hip was the leg operating speed. To mimic human walking and "human-like" uneven terrain testing the hip motor must rotate the robot's legs at 17 rpms, which is a steady walking gait for a human [2]. This speed is calculated below:

$$\frac{1 \text{ swing phase step}}{0.4 \text{ sec}} * \frac{40 \text{ deg}}{1 \text{ swing phase step}} * \frac{1 \text{ rev}}{360 \text{ deg}} * \frac{60 \text{ sec}}{1 \text{ min}} = 17 \text{ rpm}$$

This assumes an adult human walking speed of one step per second. Since the motor only rotates the legs during swing phase and the swing phase makes up only 40% of the gait cycle (the other 60% is during stance), one swing phase step takes 0.4

seconds [6]. This also assumes a leg travel of 40° from toe off to heel strike during each step [6]. According to a study, the approximate step length for an adult, age 15-19, is 66 cm (2.16 ft) [7] with a walking velocity of 135.1 cm/s (265.9 ft/min) [8]. Since the robot is modeled from a ten year old boy the robot should be capable of a step length of 61.5 cm (2.02 ft) [7] and a walking velocity of 132.3 cm/s (260.4 ft/min) [8]. These numbers do include 11-13 year olds, but provide a basis for comparison. Based on the geometry of the robot with a 28.36" length leg, rotated 30° forward and 10° backward and adding approximately 3" since the Jaywalker step length is measure from heel to mid-foot and the study uses a heel to heel measurement, the expected step length is 2.02 ft..

The independent hip drive design did not include the previous timing pulley and timing belt since they were flexible connections, so two spur gears with a gear ratio of 2:1 were added to the existing 30:1 gear train ratio to allow the legs to rotate at 17 rpm. One 24 tooth spur gear was added to each gear train shaft and one 48 tooth spur gear was attached to each outer leg driveshaft (Figure 11).

5.2 Torque Analysis

A static torque analysis was performed in order to calculate the necessary torque required at the hip to lift each outer leg forward 30° from vertical. This can be found in Appendix A and was calculated to be 70.36 in-lb. According to the torque curve supplied by the stepper motor manufacturer at 1020 rpm (17 rpm at the legs) with a 24 VDC @ 4 Amps power supply, 0.18 N-m (25.5 oz-in) of torque created [9]. Multiplying the stepper motor torque by the 30:1 gear train increases the torque to

765 oz-in or 47.81 in-lb. Multiplying again by the additional 2:1 gear ratio necessary to achieve 17 rpm increases the torque to 95.63 in-lb. This gives a safety factor of 1.36.

A 48VDC @ 4 Amps power supply was purchased for the previous ratchet/pawl hip design because the 24 VDC @ 4 Amps power supply could not supply enough torque to the single hip motor to rotate and hold both outer legs simultaneously [4]. Using the 48VDC @ 4 Amps power supply increases the stepper motor torque at 1020 rpm from 25.5 oz-in to 53.8 oz-in [9]. Multiplying the torque by the 30:1 gear train and 2:1 gear ratio the hip torque increases from 95.63 in-lb to 201.8 in-lb. Deducting 1% from this torque for the losses due to the additional spur gear meshing gives 199.78 in-lb or a safety factor of 2.8.

5.3 Spur Gear Selection

One 48 tooth, 24 DP, 14 ½° spur gear and 96 tooth, 24 DP, 14 ½° were mounted to the gear train shaft and leg driveshaft respectively. These spur gears were selected from Boston Gear (Pricing information can be found in Appendix B) because they created a 2:1 gear ratio resulting in an overall leg rpm of 17 and the 48 and 96 tooth gears had the smallest center distance of 3" to allow the best packaging. The gears were positioned with the smallest diameter gear on the gear train shaft and the largest on the leg driveshaft (Figure 11) to maximize the torque output at the leg/hip connection.

5.4 Drive Shaft Design

Each driveshaft uses four snap rings to prevent translation during leg rotation.

One snap ring was placed on each flat side of the bearing carrier (Item 1 in Figure 12)

and one against the inside race of the ball bearing (Item 2). This prevents the driveshaft from translating relative to the bearing carrier and the bearing translating relative to the bearing carrier.

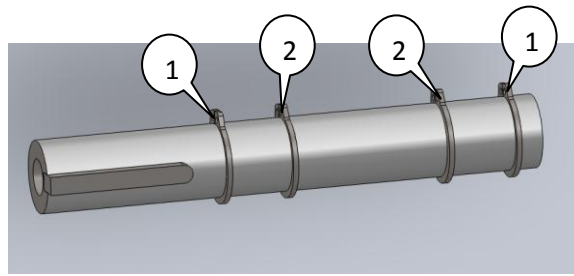


Figure 12: Snap ring locations on leg drive shaft.

5.5 Stepper Motor/Drive Shaft Mounting

The outside bearing carrier (Item 1 in Figure 13) and stepper motor mounting plate (Item 2) were consolidated to a single motor mounting plate in the independent hip drive design to reduce hardware and machining and to better align the mating gear train and leg driveshaft spur gears. Spacers were used between the gear train and motor mounting plate to align the flat faces of the spur gears to ensure they were always meshing.

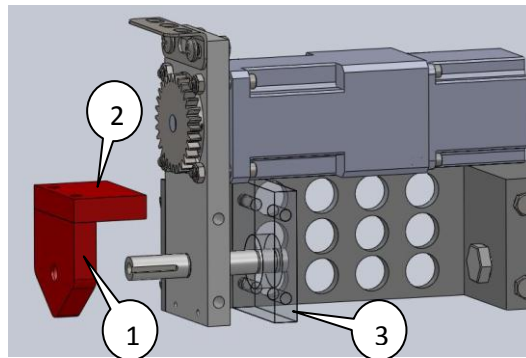


Figure 13: Top pelvis mount - removed and replaced by second bearing carrier (shown in phantom)

The meshing of the spur gears caused an interference with the existing top pelvis mount (Item 2 in Figure 13) on the original hip assembly so this mount was removed -. Removing this top pelvis mount caused a bending moment on the driveshaft due to the now cantilevered leg weight at the end of the shaft. This caused the driveshaft to be in single shear and had the potential of causing binding and extra friction as the leg rotates. To solve this, the outer bearing carrier was moved inboard (Item 3 in Figure 13) between the opposing rectangular mounting plates to support the driveshaft in two locations placing the driveshaft in double shear.

5.6 Leg Clevis Design

The outer leg clevises were designed very similar to the ratchet/pawl hip design clevises with the exception of the center three mounting holes and the recessed pockets necessary to house the ratchet/pawl assembly. The three mounting holes were removed to reduce the clevis weight (Figure 14) and to remove the weight of the hardware that previously attached the clevises together. With the addition of the two extra $\frac{1}{4}$ "-20 x 1.25" length screws used to mount the large spur gear to the leg clevises and the four screws connecting the square leg plate to the clevises, the previous three center-mounted

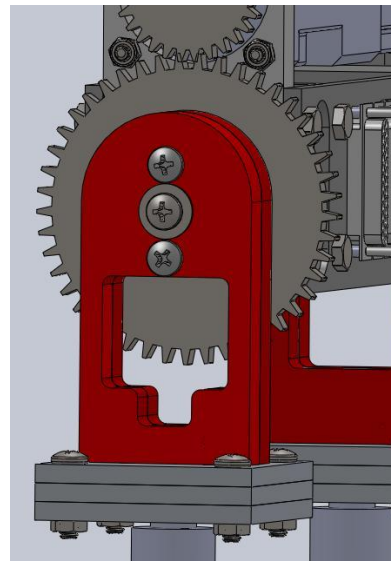


Figure 14: Weight removed from inside leg clevis

screws were unnecessary. Each outer leg clevis is designed to be keyed to its driveshaft to couple their rotations. The keystock is held inside the clevises with a 1/4-20 machine screw and washer threaded into the end of each driveshaft to prevent the keystock from vibrating out.

5.7 Packaging Concerns

In order to incorporate a secondary stepper motor and gear train assembly into the original ratchet/pawl hip design, the original motor and gear train assembly needed to be moved away from the centerline of the hip and positioned over each of the outer legs with the shafts pointing away from the centerline of the hip. After positioning the first motor and gear train assembly over the outer leg, the resulting space did not allow enough room for a second motor and gear train assembly. The length of each rectangular mounting plate had to be increased by 1.3” to allow enough room to insert the second motor and gear train assembly. This positioning allowed the removal of the original center motor mounting plate, timing pulleys, and timing belt. Removing the timing belt and timing belt allowed the single driveshaft to be removed and replaced with two smaller driveshafts, one for each outer leg.

One goal of redesigning the hip assembly was to package the electrical connections and

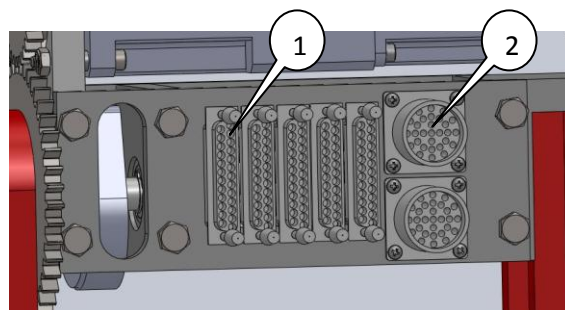


Figure 15: Organized electrical and pneumatic connectors

pneumatic hoses in a more organized way for both aesthetic reasons and to easily identify which connections control which sensors allowing easy troubleshooting when problems occur. The ratchet/pawl hip design used different sizes of D-SUB electrical connectors with varying pin quantities, different length threaded standoffs and screws to mount the connectors, random mounting locations, and dissimilar electrical wiring within the same type of electrical connectors which made troubleshooting difficult. A single 25 pin style D-SUB connector (Item 1 in Figure 15) was selected to be used throughout the entire robot to standardize components. Each D-Sub connector is designated to hold specific electric components and corresponding wiring to easily identify electrical problems. One connector is used for all accelerometers, one for encoders, and one for toe off/heel strike limit switches. The D-Sub mounting locations were integrated directly into the design of the rectangular mounting plates for two purposes. One, they eliminate unnecessary threaded standoffs and mounting screws and reduce assembly/disassembly time and secondly they remove weight from the rectangular mounting plates in order to mount the electrical connectors flush with the mounting plate surface, which reduces the overall weight of the hip. Separate electrical connectors (Item 2 in Figure 15) were used for wiring that carries larger current to prevent accidental contact and shorting with lower amp carrying wire. These connectors include the wiring for the two hip stepper motors and the three ankle stepper motors. The pneumatic hose connectors were originally mounted on two rectangular mounting plates, but are now reduced to a single mounting plate for better organization. More mounting locations for electrical and pneumatic connectors were incorporated into the design of the rectangular

mounting plates to easily add more electronics and pneumatics without remanufacturing any components.

5.8 Weight Comparison

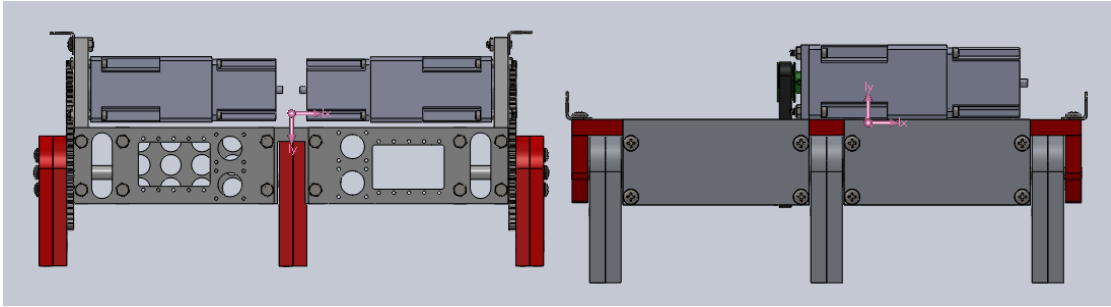


Figure 16: Weight comparison of ratchet/pawl and independent hip drive

The new hip design weighs 12.63 lbs more than the old design, 29.88 lbs versus 17.26 lbs (Figure 16). The original goal when designing the robot was to reduce the hip weight because it reduces the necessary ankle torques to realign the inertial and reaction forces [5]. A large majority of the increased weight of the independent hip drive hip compared to the ratchet/pawl hip came from the second stepper motor and gear train assembly and the second stepper motor mounting plate. These three items alone account for 10.5 lbs, which is 83% of the additional weight. Another 2.3 lbs came from adding four spur gears that couple the motor and outer legs. This is compared to the 0.28 lbs for the timing pulleys and timing belt used on the original hip design. The extra weight does raise the center of the mass by 0.53” (calculated by modeling each hip in Solidworks CAD software) but this raise in

center of mass can be justified because of the flexibility the motors and gears add by allowing each outer leg to be rotated and controlled independently.

While the entire robot weighs more, many individual parts were reduced in weight from the ratchet/pawl hip design. The rectangular mounting plates on the old design weighed 0.38 lbs and the new rectangular mounting plates that are 1.3” wider only weigh 0.31 lbs, which is a weight savings of 0.32 lbs overall. This was accomplished by removing material in the interior of the plates to mount electrical and pneumatic connections. The connections were standardized and organized on the mounting plates to allow more connections to be easily installed. The previous outer leg clevises each weighed 0.42 lbs. When the three internal screws were eliminated, the internal material could then be removed reducing the clevises the weight was reduced to 0.36 lbs each. The previous 16” driveshaft was reduced to two 3.5” driveshafts reducing the weight from 0.55 lbs to 0.36 lbs; a savings of 0.19 lbs overall.

5.9 References

- [1] Strunk, G. Parallelized Distributed Embedded Control System for 2D Walking Robot for Studying Rough Terrain Locomotion. M.F.A. dissertation, University of Kansas, United States -- Kansas. Retrieved May 20, 2012, from Dissertations & Theses @ University of Kansas. (Publication No. AAT 1483851), pg 23.
- [2] Baker, B., 2010, “Development of a hybrid powered 2D biped walking machine designed for rough terrain locomotion,” Ph.D. thesis, the University of Kansas, Lawrence, KS, pp. 18.
- [3] National Center for Biotechnology Information, U.S. National Library of Medicine. (2004). *Gait Analysis*. Retrieved from

<http://www.ncbi.nlm.nih.gov/books/NBK27235/> (last visited on March 12, 2012), Figure 6-2. 15, Apr. 2012.

- [4] Ruiz, M.. Active hip actuation for walking biped with passive option. M.E. dissertation, University of Kansas, United States -- Kansas. Retrieved February 20, 2012, from Dissertations & Theses @ University of Kansas. (Publication No. AAT 1494802), pp. 30.
- [5] Honda, “Evolution of Walking Technology – 2. Achieving Stable Walking,” at <http://world.honda.com/ASIMO/history/technology2.html> (last visited March 12, 2012).
- [6] Baker, B., 2010, “Development of a hybrid powered 2D biped walking machine designed for rough terrain locomotion,” Ph.D. thesis, the University of Kansas, Lawrence, KS, pp. 16.
- [7] Oberg, Tommy, 1993, “Basic gait parameters: Reference data for normal subjects 10-79 years of age,” Journal of Rehabilitation Research, at <http://www.rehab.research.va.gov/jour/93/30/2/pdf/oberg.pdf> (last visited on July, 6 2012), pp. 222, Table 8a.
- [8] Oberg, Tommy, 1993, “Basic gait parameters: Reference data for normal subjects 10-79 years of age,” Journal of Rehabilitation Research, at <http://www.rehab.research.va.gov/jour/93/30/2/pdf/oberg.pdf> (last visited on July, 6 2012), pp. 216, Table 2a.
- [9] Oriental Motor Product Catalog at <http://catalog.orientalmotor.com/item/all-categories/pk-series-stepping-motors/pk266m-e2-0b?&plpver=11&origin=keyword&filter=&by=prod#> (last visited July 6, 2012).

6. Manufacturing

6.1 Introduction

Aluminum was the material selected for the independent hip drive design because of its high strength to weight ratio. The material was purchased from The Yard in Wichita, Kansas USA (Pricing information can be found in Appendix B). The material was cut to length, but oversized slightly so each piece had to be squared and milled to its precise measurements. Holes, slots and pockets were milled in the Mechanical Engineering machine shop at the University of Kansas, School of Engineering using a Bridgeport mill equipped with a digital readout accurate to 0.001". Shafts were turned on a manual lathe to within 0.001" of their required dimension before sanding the tool marks smooth with small grit sandpaper until the ball bearings had a "slip fit" on the shaft. The motor mounting plates were CNC milled because of their large diameter holes and the precision needed for the depth of the ball bearing pockets.

6.2 Difficulties during Manufacturing

A problem occurred when trying to mount the small spur gear to the gear train shaft. The diameter of the clearance hole in the motor mounting plate (Appendix D) was originally sized just large enough to allow the hub of the small spur gear to rotate freely. Once the stepper motor and gear train assembly were mounted to the motor mounting plate and the spur gear was placed on the gear train shaft, the motor mounting plate prevented access for an allen wrench to tighten the set screw located

on the hub of the small spur gear to lock it against the gear train shaft.

The solution to this problem was to increase the diameter of the hole in the mounting plate to allow the spur gear to be mounted to the gear train shaft before passing the entire gear through the hole in the plate.

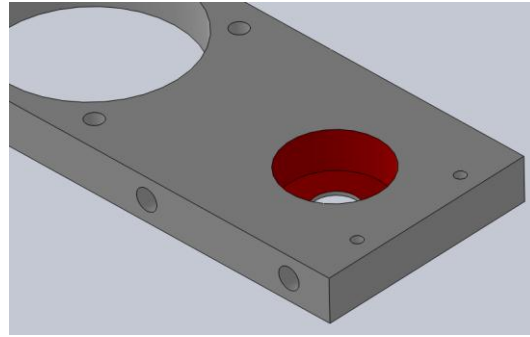


Figure 17: Bearing holes milled too deep.

The bearing holes on the motor mounting plates that were CNC milled were machined approximately 0.015" too deep (Figure 17), which made the original snap ring dimensions on the driveshafts no longer accurate. The motor mounting plates were machined before the shafts so the dimensions for the snap ring locations were adjusted to make the driveshafts still work with the deeper bearing holes. Each bearing hole depth was measured using calipers in order to determine the new snap ring locations. Because the depth of the bearing holes was slightly different between the plates, the driveshafts are no longer interchangeable. Care was taken in machining the driveshafts to make sure the bearings would not translate on the driveshaft during leg rotation. The driveshaft bearings were originally designed to be press fit into the motor mounting plates, but the drawing given to the machinist showed 1.125" +.001 / -.000. The tolerance on the bearing was actually 1.125" +.000 / -.0005. Therefore the bearing recess should have been machined with a boring bar instead of a 1.125" end mill. Because care was taken to make sure the snap rings were in the correct locations, the bearing no longer needed to be press fit.

A minor error occurred during CNC machining of the gear train mounting holes when a countersink drill bit was used during CNC machining. The length of the minor diameter of the tool was too small which causes the tool to countersink before the minor diameter had completely passed through the plate thickness creating a small countersunk hole. This did not prevent the gear train from mounting flush against the mounting plate, but is only an aesthetic error.

The two encoder mounting holes were not CNC machined with the other features on the motor mounting plate because the precise center to center distance was not given on the drawing from the manufacturer. To prevent remanufacturing the motor mounting plates due to the measured center to center distance being slightly off, the encoder mounting holes were drilled and tapped by hand. The position of the holes were determined by placing the shaft through the hole in the

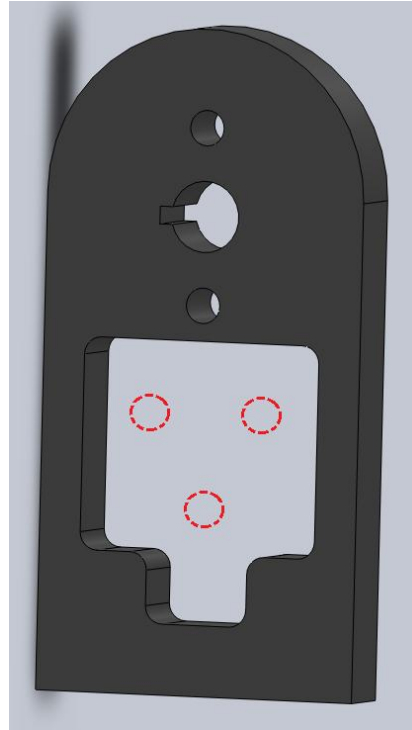


Figure 18: Weight removed from leg clevis due to machining error.

motor mounting plate and placing the encoder housing on the shaft so it laid flat on the motor mounting plate surface. The encoder housing was oriented vertically and a center punch was placed into each mounting hole and hit with a hammer to transfer the mounting holes locations on the motor mounting plate. The plate was then fixed in a vice attached to a mill with a drill chuck attachment, and a center drill was tested repeatedly in the X and Y directions to verify the tip of the center drill rested in the center punched indentation on the plate. Each hole was drilled with a #43 (.089") drill bit and threaded with a 4-40 tap. Because of the small diameter of the drill bit and the 0.5" hole depth, the resulting holes were not perpendicular to the surface even though care was taken not to drill too fast through the plate. This caused some difficulty mounting the encoder assembly, but it eventually laid flush against the plate.

The leg clevises were originally designed to have three threaded holes (phantom holes in Figure 18) in the interior of the clevis for attaching the two clevises together. The threaded callout was not placed on the machine drawing given to the CNC machinist and the holes were drilled through. This mistake allowed sufficient material to be removed from the interior of the clevises to reduce weight after a simple stress analysis was performed (Appendix C).

The broaching performed on the clevises to create the keyways was not able to be performed on the CNC mill when the other clevis features were machined. Each keyway was individually broached manually with an arbor press, broach, and a collared keyway bushing (pricing information can be found in Appendix B). This meant “eyeballing” the 90° angle of the keyway on each clevis individually. This created misalignment issues when the clevises were placed on the driveshaft, the ¼”-20 x 1.25” machine screws placed into the mounting holes and the keystock was fed into the keyway. This problem was solved by trimming down the keystock length from 1” to 0.5” so the keystock only feeds through one clevis instead both. This key length is still sufficiently strong as seen in the shear stress calculations in Appendix E. With the 1” length key the average shear stress in the keystock is 9000 psi. When the length is decreased to 0.5” the average shear stress increases to 18,000 psi. The yield stress of the 1018 keystock is 55,000 psi which gives a safety factor of 3.1.

The center U-support originally had eight ¼”-20 blind holes. When drilling the holes, it was discovered that because the four holes on the front were a mirror image of the four holes on the back, four holes could be drilled through the front face of the support and through the parts entire thickness. This would decrease

manufacturing time, allow the holes to be quickly and easily threaded, and would decrease the chance of hole misalignment by unfixturing the piece, rotating 180°, refixturing, and machining the four additional holes on the back surface. The four through holes also reduce the overall weight of the part.

The snap ring grooves on the driveshafts were difficult to machine because of the accuracy needed to prevent driveshaft translation and slop. If the distance between the outer most snap ring grooves were machined larger than specified, the driveshaft would translate and vibrate during walking and would affect foot position accuracy. Because the outer race of the ball bearings is not press fit into the motor mounting plate, they would also translate and vibrate along with the driveshaft. If the distance between the snap ring grooves were machined too small, the shaft the snap rings would interfere with the outside flat faces of the bearing carriers and the driveshaft would have to be re-machined. If the distance between the inside snap ring groove locations were too small, the bearings would unseat from the inside face of the bearing carrier and would translate and vibrate along the driveshaft during walking and if the distance was too large the snap rings would interfere with the bearing carriers and the driveshaft would have to be re-machined. The snap ring groove tool also added difficulty because it did not fit in the standard lathe tool post for the lathes equipped with a digital readout. This meant using the markings on the lathe carriage hand wheel, which took more time to machine.

6.3 Manufacturing Improvements

FEA software could be used in the future to reduce part weights. Simple calculations were performed to reduce part weights, but more weight can be eliminated by applying force sensors or strain gauges to the robot during testing and analyzing stresses during real-time operation and factoring these in the FEA part analyses.

It would have been useful to have a CNC mill that had the ability to broach keyways while the part was still fixed in the vice. The mill did not have this ability so the keyways for each outer leg clevis had to be broached by hand separately using a keyway bushing and an arbor press. Care was taken to line up each keyway so when the two outer leg clevises were mounted together the keyways would line up. This was the case for one set of outer leg clevises, but the keyways for the other set did not line up. Instead of machining a brand new set of outer leg clevises, the keystack was cut in half so it only passed through one outer leg clevis instead of both as originally designed.

In future versions, the pairs of outer leg clevises could be reduced to a single outer leg clevis to reduce weight. This was not implemented in this design because of the concern for off-center loading caused by the impact of the feet during testing. Future investigation may determine that this is not a problem and a single outer leg clevis can be used.

Guarding should also be designed to surround the meshing spur gears on both sides of the hip for safety. The meshing spur gears could cause serious injury if a

hand, finger, or piece of clothing where to get too close during operation or when performing maintenance.

7. Assembly

7.1 Introduction

After all parts were machined the robot was assembled. First, the two center leg clevises were placed into the center U support, the holes were lined up and the $\frac{1}{2}$ " bolt inserted. The washers and jam nut followed. Next the four pelvis mounting plates were mounted onto the center U support with eight $\frac{1}{4}$ "-20 hex cap screws. A snap ring was placed on each driveshaft in the groove furthest from the threaded end. One bearing carrier and ball bearing assembly were placed onto the driveshaft oriented so the snap ring was flat against the flat side of the bearing carrier. A second snap ring was placed on the driveshaft against the bearing inner race to lock the assembly in place. A third snap ring was placed into the next groove followed by the motor mounting plate and ball bearing assembly and a fourth snap ring to lock the motor mounting plate in position. These entire assemblies were then mounted to the four pelvis mounting plates with sixteen $\frac{1}{4}$ "-20 hex cap screws. Each pair of outer leg clevises were then mounted to a 48 tooth spur gear with two $\frac{1}{4}$ "-20 hex screws and then assembled on the driveshaft against the surface of the snap ring. The 24 tooth spur gear was placed onto the gear train shaft and locked in place with the provided set screw. The gear train was mounted to the stepper motor with four 4mm socket head screws and then each spur gear/stepper motor/gear train assembly were mounted on a motor mounting plate with four 10-24 socket head screws making sure to mesh the 24 and 48 tooth spur gears before tightening the screws. Each keystick was placed in the keyways of the shaft and outer leg clevises and held in place with a $\frac{1}{4}$ "-

20 x ½” hex cap screw and washer threaded into the driveshaft end. The D-Sub connectors and pneumatic connectors were then mounted onto the pelvis mounting plates and the wiring and hoses were routed.

7.2 Difficulties during Assembly

Difficulties during assembly occurred when placing the snap rings in the driveshaft grooves. First, a snap ring was placed in the driveshaft groove furthest from the threaded end. Then, the bearing carrier and ball bearing assembly were slid onto the driveshaft followed by a second snap ring. The second snap ring was difficult to position flat against the ball bearing inner face to seat into the groove on the driveshaft because the groove distance from the driveshaft end was slightly undersized. After the driveshafts were attached to the bearing carriers and rotated the steel snap rings rubbed against the flat faces of the aluminum bearing carriers and scratched the surface. To prevent further scratching and wear, 0.001” thick steel washers were placed between the snap rings and bearing carrier surface.

Assembling the center leg clevises and center U-support were difficult because of the small differences between the thicknesses of the center leg clevises and center U-support slot to prevent slop. Because of the close dimensions, the ½” bolt was difficult to slide through the center U-support, through each of the center leg clevises and into the other hole in the center U-support. To solve this problem, the center U-support and center leg clevises could be combined into a single part eliminating the ½” bolt, washers, and jam nut. This is possible because there is no relative motion between the parts and this would reduce overall weight and cost.

8. Test Methods

8.1 Test Method for Robot Range of Motion

The robot must have the same or better range of motion than a human to operate within the human walking gait parameters. This means being able to rotate each leg forward at least 30° and backward at least 10°. The robot will be tested with its knee flexed to mimic its swing leg during walking and with its knee extended to maximize the motor torque. This testing will ensure the independent hip drive allows the robot to operate within the human walking gait parameters for both possible walking conditions.

8.2 Test Method for Open Loop Stable Step Length

After the range of motion is proven the robot must be capable of taking an open loop stable step. This is necessary to tune the robot's controller for a consistent stable step length. With the previous ratchet/pawl hip the open loop stable step length was 5 1/2" [1]. The bipedal robot will attempt to increase this step length to achieve a more realistic 10 year old boy step length of 61.5 cm (2.02 ft, 24.4") [2]. The Jaywalker screen shots for this test can be seen in Appendix F.

8.3 Test Method for Robot Walking at Human Gait Parameters

The robot's motor must be capable of operating the robot's legs at 17 rpm to be within human walking gait parameters. This will be tested to ensure the robot's motor can operate the legs at this rpm.

8.4 References

- [1] Strunk, G. Parallelized Distributed Embedded Control System for 2D Walking Robot for Studying Rough Terrain Locomotion. M.F.A. dissertation, University of Kansas, United States -- Kansas. Retrieved May 20, 2012, from Dissertations & Theses @ University of Kansas. (Publication No. AAT 1483851), pg 45.

- [2] Oberg, Tommy, 1993, "Basic gait parameters: Reference data for normal subjects 10-79 years of age," Journal of Rehabilitation Research, at <http://www.rehab.research.va.gov/jour/93/30/2/pdf/oberg.pdf> (last visited on July, 6 2012), pp. 222, Table 8a.

9. Test Results

9.1 Robot Range of Motion

Testing has shown that the Jaywalker is capable of rotating its legs forward and backward to a maximum of 50° with its knee flexed and to 45° with its knee extended before the motors started to back drive [1]. This proves the robot can operate within the human gait range of motion.

9.2 Test Results for Open Loop Stable Step Length

Testing has shown that the Jaywalker can successfully take an open loop step of 7.5" using the independent hip drive. This is a 36% longer step than the 5 1/2" step that could be achieved by the ratchet/pawl hip design [1].

9.3 Test Results for Robot Walking at Human Gait Parameters

Testing has shown the Jaywalker's motor controller is capable of rotating its legs at 17 rpm with two ramping steps under 0.25 seconds [1]. This time is within the swing leg time period of 0.4 seconds so the robot is capable of operating within human walking gait parameters [2].

9.4 References

- [1] Strunk, G. Parallelized Distributed Embedded Control System for 2D Walking Robot for Studying Rough Terrain Locomotion. M.F.A. dissertation, University of Kansas, United States -- Kansas. Retrieved May 20, 2012, from Dissertations & Theses @ University of Kansas. (Publication No. AAT 1483851), pg 41-45.

- [2] Baker, B., 2010, "Development of a hybrid powered 2D biped walking machine designed for rough terrain locomotion," Ph.D. thesis, the University of Kansas, Lawrence, KS, pp. 7.

10. Conclusions

The Jaywalker is being developed with an active hip in order to study how well it traverses uneven terrain. The addition of a secondary hip motor has allowed the Jaywalker to control each of its outer legs independently and has increased its step length accuracy by 1) removing all flexible transmission connections and coupling the motors directly to the leg driveshafts; 2) reducing leg position errors due to the ratchet/pawl mechanism skipping teeth during engagement; and 3) increasing the leg rotation resolution by eliminating the ratchet/pawl mechanism and using the 0.09 deg/step resolution of the motor and micro-stepping controller.

From testing, the robot is capable of operating at the human walking gait of 17 rpm, can achieve the same leg range of motion as a human, and can take a 36% larger open loop step compared to the previous ratchet/pawl hip design. The design is considered a success and will allow more in depth testing to be performed on uneven terrain.

11. Future Recommendations and Testing

Recommendations to improve the Jaywalker include:

- 1) Performing FEA analysis on hip components to reduce individual part weights based on forces experienced during testing.
- 2) Integrate logic into the robot's control system to tell the robot how it should attempt to re-stabilize itself during different instable situations.
- 3) Perform testing on uneven terrain using simple shapes like blocks and dowel rods to identify the robot's strengths and weaknesses. Make adjustments to the control system based on findings.
- 4) Include passive hip option because it saves energy and better mimics human motion.

In the future the Jaywalker should have built-in logic to decide how it should react to different instable situations. One method that can be programmed into the Jaywalker's control system is the "extrapolated center of mass" method developed by Hof [2]. This method uses equations developed from the inverted pendulum model to determine the dynamic stability of the robot in real-time.

$$x_0 + (v_0/\omega_0) \leq u \quad (1)$$

Equation (1) was developed by Hof, where x_0 is the perpendicular distance from the center of mass (COM) to the ankle shaft, v_0 is the initial horizontal velocity of the COM, $\omega_0 = \sqrt{g/l}$ where g is the gravitational constant and ' l ' is 1.24 times the trochanteric height [2]; and u is the perpendicular distance from the center of

pressure (CoP) to the ankle shaft (Figure 19). The CoP can be calculated from Equation 2 where $\text{velocity}_{\text{CoP}}$ is the initial velocity of the CoP before the imbalance.

$$\text{CoP} = x - (\text{velocity}_{\text{CoP}} / (\omega_0)^2) \quad (2)$$

This equation uses the assumptions that (1) the robot's balance is described only by the movement of the robot's COM, (2) the distance from the robot's COM, l , to the robot's ankle remains constant, (3) COM deviations are small compared to the distance ' l '. This analysis can

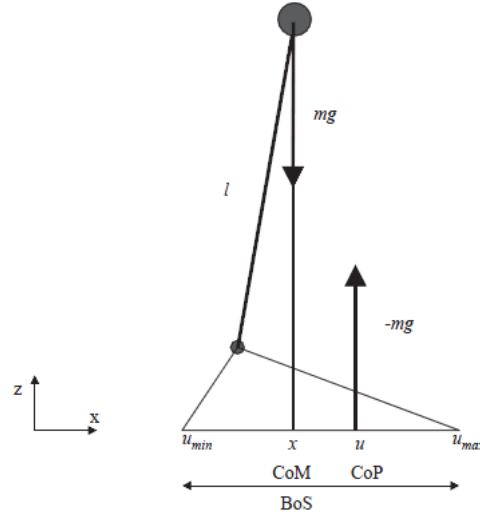


Figure 19: Free body diagram of IPM [2].

be used as a tool to predict whether the robot will become unstable after encountering a perturbation by utilizing the robot's microprocessor to constantly evaluate its COM position and make sure it never exceeds the CoP position [2].

An initial velocity of 1.65 ft/sec should be used during testing, which comes from a 1 step/sec average human walking speed and calculating the arc length the swing leg travels in 40° using a leg length of 28.36".

$$\frac{1 \text{ step}}{1 \text{ sec}} * \frac{(40^\circ/360^\circ) * 2 * \pi * (28.36''/12)}{1 \text{ step}} = 1.65 \text{ ft/sec}$$

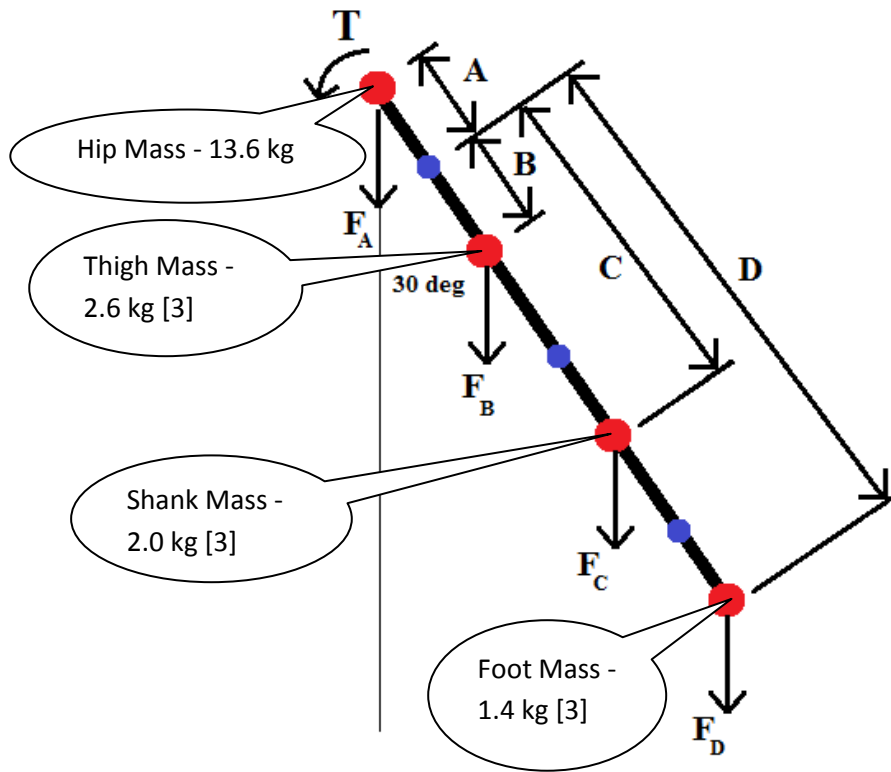
The initial velocity should be introduced to the robot by a weight and pulley system. A cable should be attached to the robot hip and ran through a series of pulleys before attaching to a weight hanging above the ground. When the quick release is triggered, the weight should drop to the ground pulling the robot hip forward and simulating a velocity impulse. The height and mass of the hanging weight should be calculated using the impulse formula $m_1 * g * t = m_2 * v$ where m_1 is the mass of the hanging mass, m_2 is the weight of the robot, g is the gravitational constant, t is the time it takes for m_1 to hit the ground and v is 1.65 ft/sec. The value 't' should be used to calculate the required height of the hanging mass using the projectile motion equation $d = v_i * t + \frac{1}{2} * a * t^2$.

The success criteria for this test should be both visual (i.e. whether the robot falls over) and experimental by determining if the trial meets the stability criteria of the “extrapolated center of mass” equation. Based on Hof’s analysis the following equation must be satisfied for stability:

$$x_0 + (v_0/\omega_0) \leq u \quad \text{Equation (3)}$$

Where v_0 is the initial COM velocity, ω_0 is $\sqrt{g/l}$. As long as the CoP distance is always greater than the COM distance the robot is capable of correcting its instability.

Appendix A –Maximum Motor Torque to Raise Hip to 30°



$$\Sigma T = 0 = -F_B \cdot \sin(30^\circ) \cdot B - F_C \cdot \sin(30^\circ) \cdot C - F_D \cdot \sin(30^\circ) \cdot D + F_A \cdot \sin(30^\circ) \cdot A + T$$

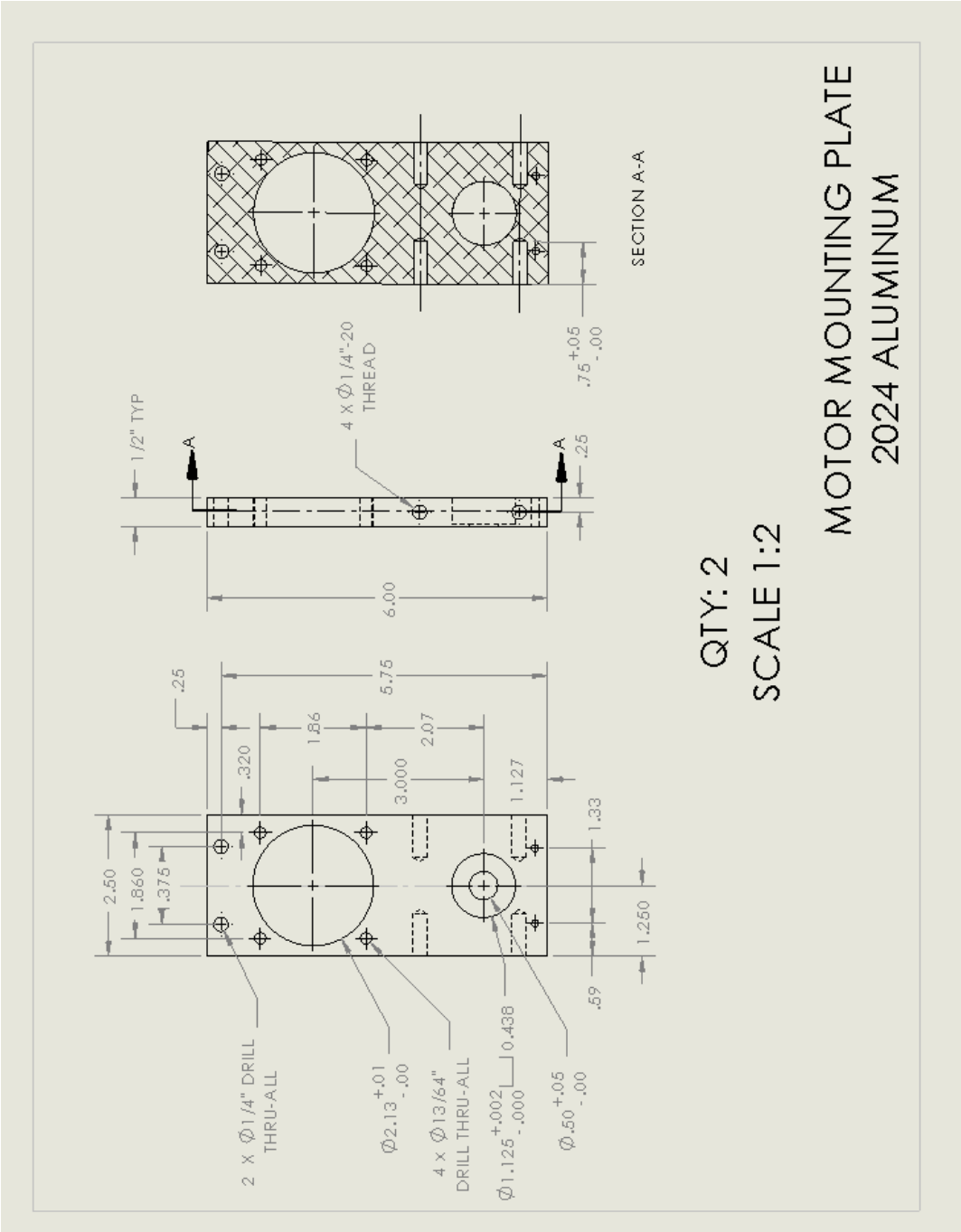
$$\Sigma T = 0 = - (2.6) \cdot (9.81) \cdot \sin(30^\circ) \cdot B - (2.0) \cdot (9.81) \cdot \sin(30^\circ) \cdot C - (1.4) \cdot (9.81) \cdot \sin(30^\circ) \cdot D + (13.6) \cdot (9.81) \cdot \sin(30^\circ) \cdot A + T$$

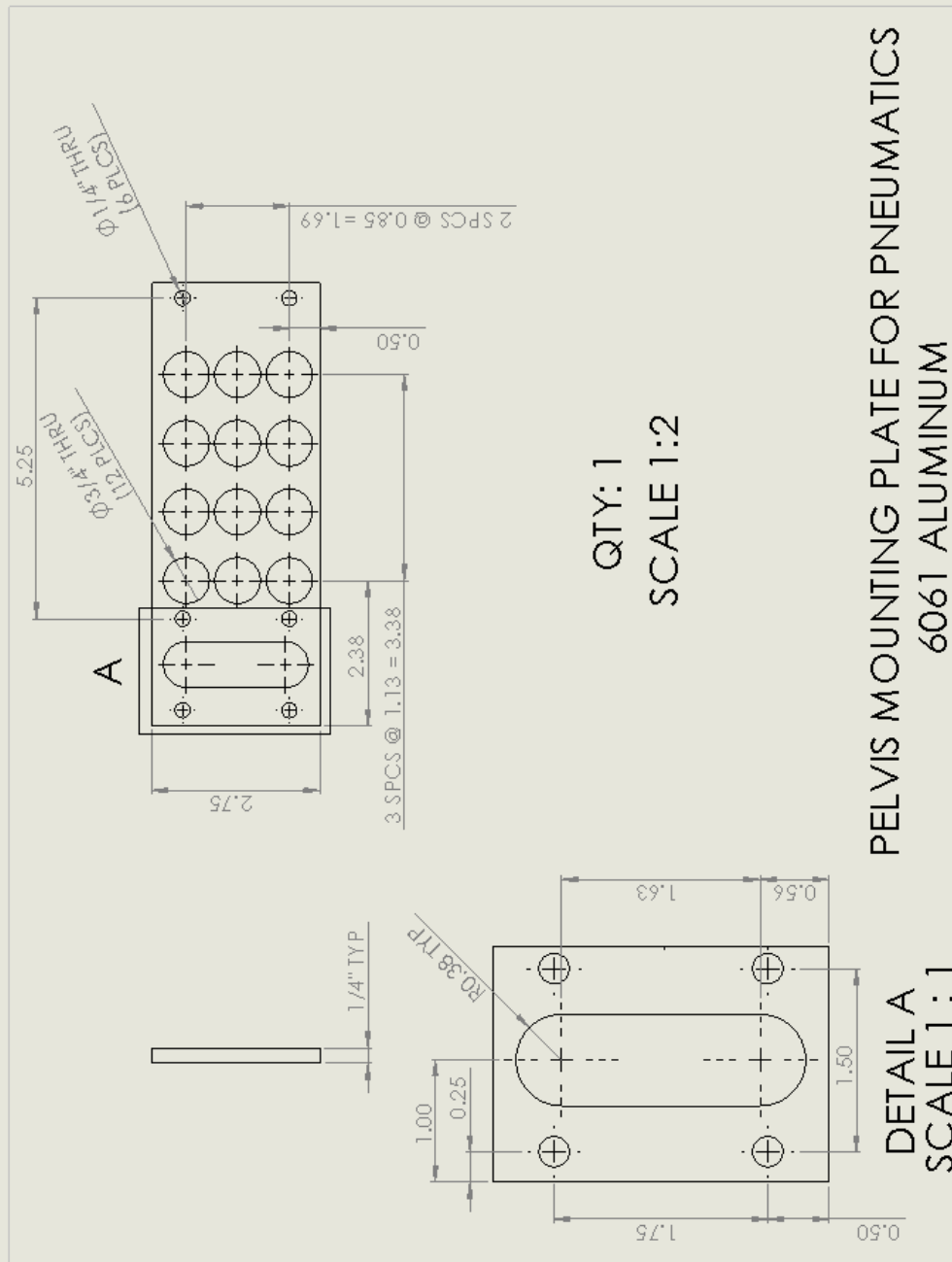
$$\Sigma T = 0 = -25.5\text{N} \cdot (0.5) \cdot 0.072\text{m} - 19.6\text{N} \cdot (0.5) \cdot 0.582\text{m} - 13.7\text{N} \cdot (0.5) \cdot 0.720\text{m} + 133.4\text{N} \cdot (0.5) \cdot 0.054\text{m} + T$$

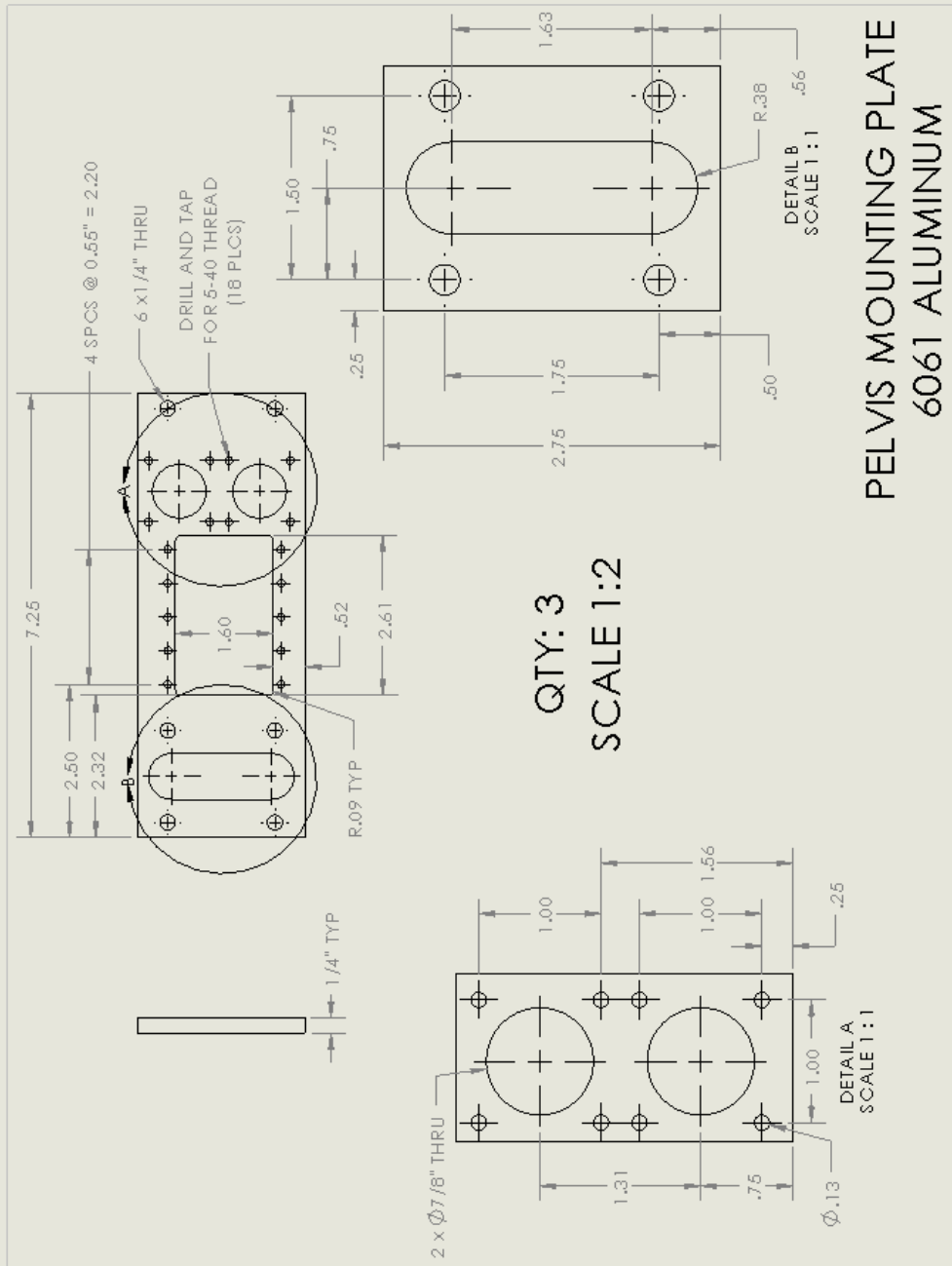
$$T = 7.95 \text{ N-m} = \mathbf{70.36 \text{ in-lb}}$$

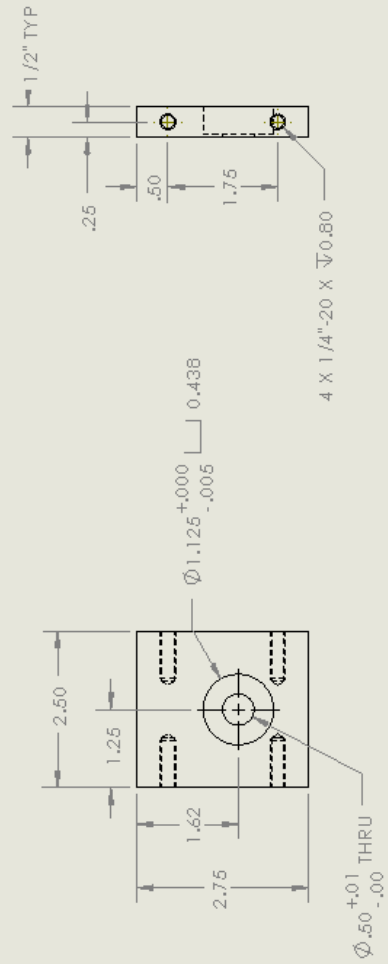
Appendix B –Bill of Materials

Description	Qty	Price	Extended Amount
Aluminum Plate			
1/2" x 3" x 5.75" 2024 plate	2	2.25	\$ 4.50
1/2" x 3" x 4.75" 2024 plate	4	2.00	\$ 8.00
1/2" x 3" x 4.875" 2024 plate	2	2.00	\$ 4.00
1/2" x 3" x 2.75" 2024 plate	2	1.50	\$ 3.00
1/4" x 3" x 7.25" 2024 plate	4	1.75	\$ 7.00
2 3/4" x 2 3/4" x 3" 2024 plate	1	5.00	\$ 5.00
Shipping	1	15.75	\$ 15.75
Spur Gears			
Pitch Diameter (in)			
Pitch Diam.: 2", Bore: 0.375"	2	\$ 24.35	\$ 48.70
Pitch Diam.: 4", Bore: 0.5"	2	\$ 51.27	\$ 102.54
Ball Bearings			
OD: 1.125", Thickness: 0.375"	4	\$ 6.90	\$ 27.60
Hardware			
HHCS 1/4"-20 x 0.5" LGTH	26	\$ 0.48	\$ 12.48
AHMS 10-24 x 1 1/4"	8	\$ 0.51	\$ 4.08
AHMS M4 x 16 MM LGTH	8	\$ 0.09	\$ 0.72
Shoulder Screw 1/2-13, 6" LGTH	1	\$ 4.27	\$ 4.27
Steel Shim 1/2" ID, 3/4"OD, 0.001" Th	1	\$ 4.31	\$ 4.31
Key Stock 1/8"x 3/16" x 12"	1	\$ 1.32	\$ 1.32
Retaining Ring for 1/2" Diam Shaft	1	\$ 8.94	\$ 8.94
Machining			
Keyway Bushing for Broach 1/2" Diam	1	\$ 9.85	\$ 9.85
Shim for Keyway Broach 1/8" keyway	1	\$ 2.49	\$ 2.49
Two-Flute End Mill 1/8" Diam	1	\$ 11.71	\$ 11.71
Grooving Tool for Retaining Ring 0.039"	1	\$ 41.45	\$ 41.45
Grand Total			\$ 327.71



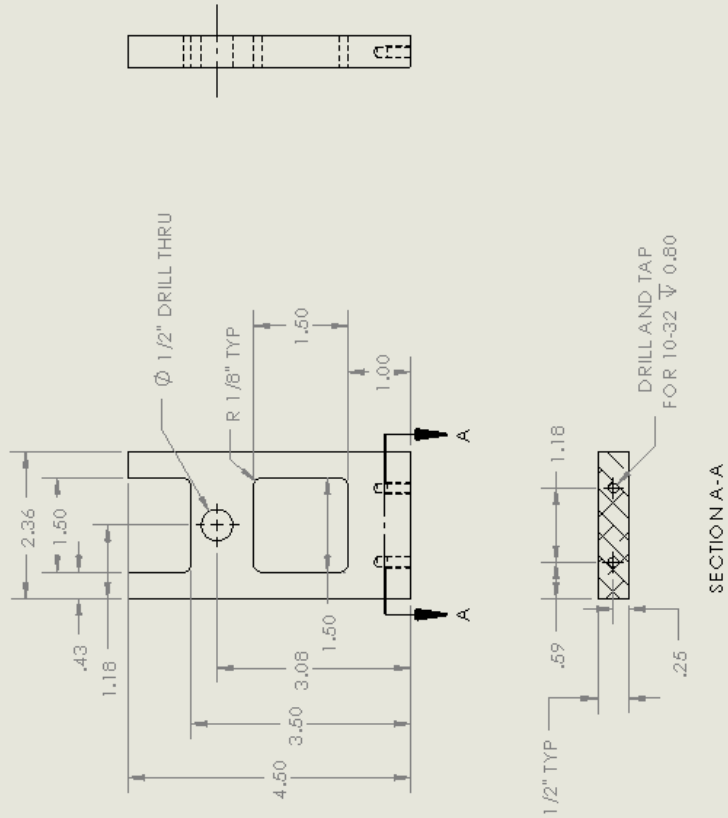






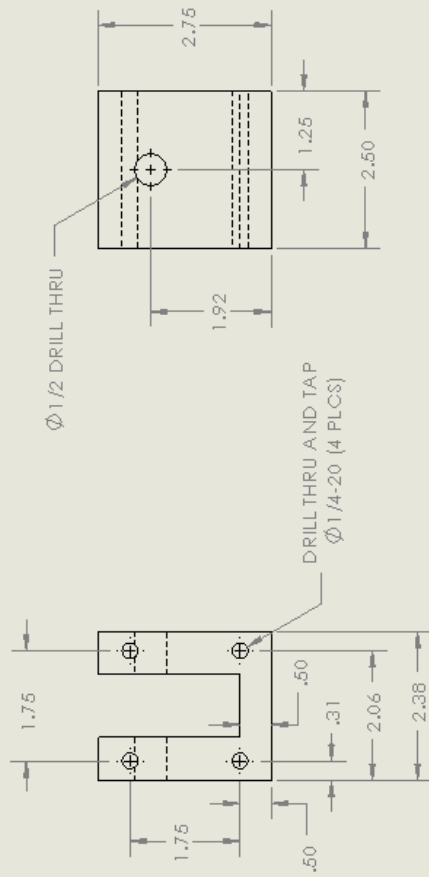
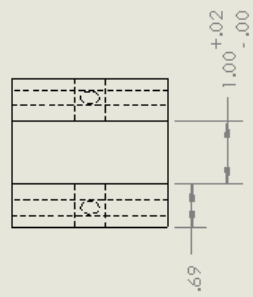
QTY: 2
SCALE 1:2

BEARING CARRIER
6061 ALUMINUM



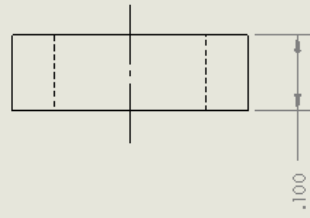
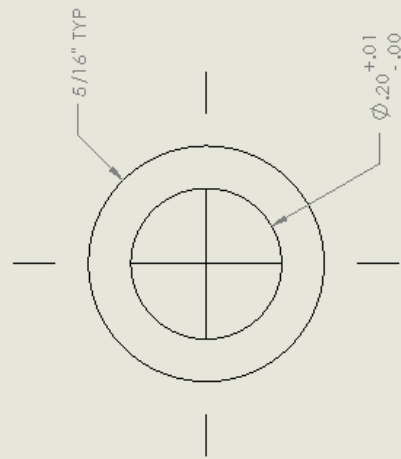
QTY: 2
SCALE 1:2

CENTER LEG CLEVIS
6061 ALUMINUM



QTY: 1
SCALE 1:2

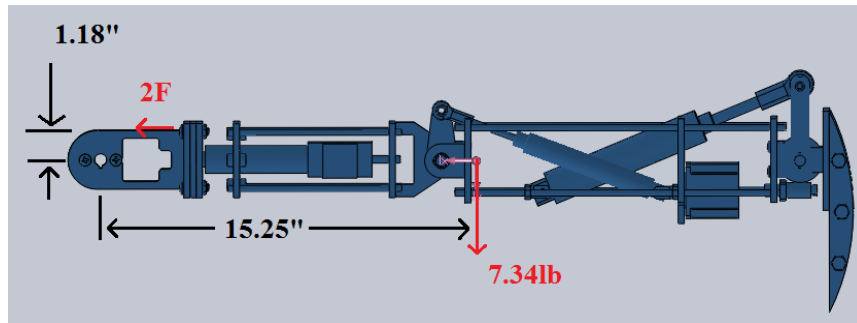
CENTER LEG U-SUPPORT
6061 ALUMINUM



QTY: 8
SCALE 6:1

GEARTRAIN SPACER
A36 STEEL TUBE

Appendix D –Stress Analysis for Leg Clevis Weight Reduction



Material was removed from the leg clevis after performing a simple normal stress analysis. Force 'F' is calculated by summing the moments about the axle. The moment about the axle caused by the leg's mass is being counteracted equally by the two wall thicknesses of the leg clevis (one side in tension the other in compression).

Both of these "F" forces sum to a 2F.

$$\Sigma T = 0 = 2F (1.18") - 7.34 \text{ lb} (15.25")$$

$$F = 47.43 \text{ lb}$$

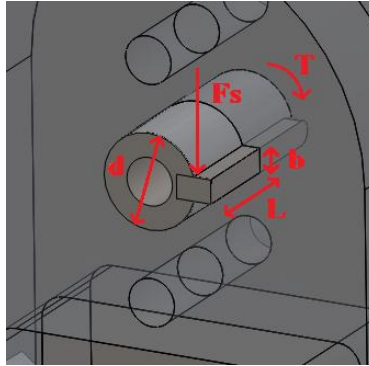
$$\sigma = F/A = 47.43 \text{ lb} / (.305" \times 0.5") = 311 \text{ psi}$$

The yield stress of 2024 Aluminum is 11,000 psi resulting in a safety factor of 35.

The leg clevis wall thickness necessary to cause failure in bending would be approximately 1/64", which is almost 39 times smaller than its current thickness.

Future analyses can use finite element analysis to reduce the part weights even further.

Appendix E –Keyway Shear Stress Analysis



Shear force applied to a keystock is calculated using the following equation [1]:

$$F_s = T / (d/2)$$

Where 'Fs' is the shear force in lb_f, 'T' is the torque applied to the shaft in in-lb_f, and 'd' is the diameter of the shaft in inches.

Shear Stress of the keystock is calculated by dividing the shear force by the keystock area.

$$\tau = F_s / (L * b)$$

Where 'τ' is the shear stress in psi, 'L' is the length of the key and 'b' is the width of the keystock. The shear stress is compared with the yield stress of the keystock material to determine if the keystock length is sufficient.

With a 1" length keystock in outer leg

$$F_s = T / (d/2) = 281.25 \text{ in-lb} / (0.5"/2) = \mathbf{1,125 \text{ lb}}$$

$$\tau = F_s / (L * b) = 1125 \text{ lb} / (1" * 1/8") = \mathbf{9,000 \text{ psi}}$$

Yield Stress of 1018 keystock is 55,000 psi, Factor of Safety: 6.1

With a 1/2" length keystock in outer leg

$$\tau = F_s / (L * b) = 1125 \text{ lb} / (0.5" * 1/8") = \mathbf{18,000 \text{ psi}}$$

Even with the reduced keystock length Factor of Safety: 3.1.

Appendix F – Jaywalker Step Test Screenshots

Still shots for every third frame of video taking during one test of the middle leg showing toe off (Frame 1) to heel strike (Frame 13) [1].



1



2



3



4



5



6



7



8



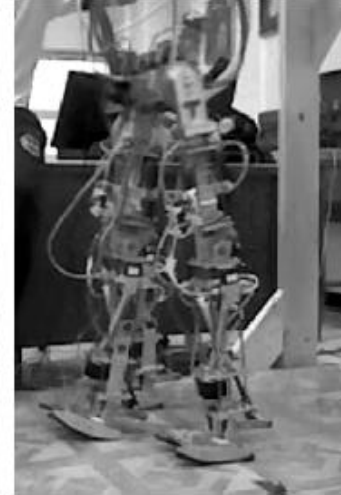
9



10



11



12



13

Appendix G: Appendix References

- [1] Strunk, G. Parallelized Distributed Embedded Control System for 2D Walking Robot for Studying Rough Terrain Locomotion. M.F.A. dissertation, University of Kansas, United States -- Kansas. Retrieved May 20, 2012, from Dissertations & Theses @ University of Kansas. (Publication No. AAT 1483851), pgs 92-93.
- [2] Hof, A. L., Gazendam, M. G. J., and Sinke, W. E., 2005, "The condition for dynamic stability," *Journal of Biomechanics*, 38(1), pp. 1-8.
- [3] Baker, B., 2010, "Development of a hybrid powered 2D biped walking machine designed for rough terrain locomotion," Ph.D. thesis, the University of Kansas, Lawrence, KS, pp. 51.